CONTROL OF TEXTURE IN MONOLITHIC ALUMINA

David Brandon*, Dezhou Chen and Helen Chan

Department of Materials Science & Engineering
and
Materials Research Center
Lehigh University
Bethlehem, PA 18015

Abstract

Conventional ceramic powder slips seeded with α-Al_2O_3 platelets were rheologically processed to align the seed crystals. An aqueous-based gel reaction was used to ensure that alignment was retained in the green body and throughout the drying procedure. Bulk samples were produced by laying-up the cast tapes, filter pressing to form a green compact, and then drying and sintering. The degree of preferred orientation in the sintered samples was characterized by X-ray diffraction. It was found that the degree of texture was significantly enhanced relative to samples processed in the same manner, but with no platelet additions. SEM study of the final microstructures showed that the grain size and grain morphology was sensitive to the initial distribution of platelets within the green tape, which in turn was dependent on the volume fraction and size of the platelets. Further, it was demonstrated that using this technique it is possible to achieve a specimen which exhibits an equi-axed grain structure, and yet has a strong degree of preferred orientation. Finally, studies of indentation cracking showed that a pronounced texture inhibited long range crack propagation, and instead promoted localized cracking.

* Presently on leave from the Technion - Israel Institute of Technology, Haifa 32000, Israel

Introduction

Recently, there have been a number of studies aimed at aligning particulate reinforcement during the processing of a ceramic slip [1-14]. Clearly, reinforcement phases in the form of whiskers or platelets readily lend themselves to these types of processes. In the case of structural ceramics, SiC whiskers dispersed in an aqueous alumina slip containing a polysaccharide have been aligned by extrusion into a gelling solution. The resultant flexible fibre has been filter-pressed, dried and sintered to yield a product with improved toughness and strength [1,2]. A slip based on alumina platelets has also been processed into a 'layered' monolithic alumina which exhibited exceptional bend strength when sintered to final density [3]. In an analogous study, Carisey et al. reported a modified tape-casting process, in which the shear forces beneath an extended 'doctor-blade' were used to align dispersed alumina platelets (2 to 20 vol% of the total solids content of the slip) [4]. A gelling reaction in aqueous solution was used to preserve the alignment, and the wet, flexible tape was layed up and filter-pressed prior to drying and sintering. It is the specimens made by this last process which are the subject of the work reported here.

Prior to the development of the gel-casting process, attempts were made to achieve platelet alignment using more conventional tape-casting technology in which the sol-gel transition on exiting from the 'doctor-blade' is achieved by a combination of monomer polymerization and solvent evaporation [5]. Although thin samples could be successfully produced by this process, the large amount of organic additives (20 vol.% or more), and the consequent limitations on sample integrity during 'burn-out' of these additives, made it impossible to produce samples thick enough for conventional mechanical testing.

The microstructure and mechanical properties of gel-cast alumina products manufactured by the lay-up of tapes containing aligned Al_2O_3 platelets have been reported previously [15]. The final structure consists of non-equiaxed, platelike grains, and has a very strong preferred orientation (texture) with the c-axis perpendicular to the plane of the gel-cast tape. The bend strength is relatively high (500 MPa), as is the fracture toughness (5 $MPa.m^{1/2}$). These values are comparable to what one would expect for an untextured alumina of similar grain size ($>10\mu m$) [16].

In alumina, the thermal anisotropy is such that the value of the expansion coefficient parallel to the c-axis exceeds that perpendicular to the c-axis by 10%. Perhaps not surprisingly, therefore, a strong c-axis texture has been shown to give a large reduction in the residual thermal stresses when compared to a conventional monolithic alumina (typically by a factor of about 3) [15]. In the present paper we examine the microstructural and crystallographic features which characterize textured monolithic alumina using specimens derived from the work reported previously [4,15].

Experimental Procedure

All samples were produced[1] by the modified aqueous tape casting process previously described [4]. The alumina platelets were supplied by Elf Atochem (France) in three sizes: 3-7 μm, 10-15 μm and 15-25 μm. The polysaccharide used was sodium alginate, and the minimum quantity required to gel the slip varied from 1.0 to 2.0 wt.%, depending primarily on the gelling cation. Between 2 and 20 vol.% of the solids content of the slip was in the form of platelets, while Sumitomo AKP50 high purity alumina powder accounted for the remainder. The path length for Couette flow under the extended 'doctor-blade' was 40 mm, while the blade gap was adjusted to between 0.25 and 2.5 mm. The tape exiting from the 'doctor-blade' was wetted with a flowing aqueous solution of gelling cation which diffused through the tape thickness. Different gelling cations varied greatly in their ability to affect the gel-reaction speed, and the time required to complete gelling (typically 2 to 20 min). In all, six gelling cations were tested. The mechanical strengths of the gels was dependent on the nature of the gelling ion, and varied in the order:

$$Ba^{2+} > Sr^{2} > Ca^{2+} > Ce^{4+} > Y^{3+} > La^{3+}$$

The flexible wet tapes were stripped from the Teflon substrate and washed to remove excess cation. The tapes were then sectioned, layed up and filter-pressed, before being dried and sintered. The sintering schedule comprised three stages: burn-out of the organic additives at 600°C for 2 hrs., stabilization of the interconnected pore structure at 900°C for 17 hrs., and sintering to final density at 1475 to 1550°C for 3 to 15 hrs. Samples made from 10 layers of gel-cast tape typically had final dimensions of 26 x 26 mm and a thickness of 3-5 mm. The

per ltr

[1] Samples were processed in the Dept. of Materials Engineering at the Technion, Haifa, Israel.

sintering shrinkage was anisotropic, as would be expected from the constraints associated with the aligned platelets.

The results reported here refer primarily to specimens which were Ca and Sr gelled; the samples also contained varying amounts of Mg and Cr as sintering additives. Calibrated secondary ion mass spectroscopy (SIMS) indicated that the combined Mg and Cr did not exceed 75 ppm, while the residual gelling cation content did not exceed 200 ppm. In the case of Sr, there was some evidence from scanning electron microscopy (SEM) that a second phase was present in the samples. The extent of preferred orientation in the samples was characterized by X-ray diffraction, together with SEM investigation of the microstructural texture (i.e., alignment of non-equiaxed grains). Finally, some limited studies were carried out on indentation cracking and fracture path.

Specimens for indentation cracking were prepared by diamond polishing, while specimens for SEM were prepared by polishing and thermal etching at 1450°C. The 15 x 15 mm square specimens for the X-ray preferred orientation study were mounted at a fixed angle in a standard X-ray diffraction (XRD) specimen mount using a special jig (Fig. 1a). The geometry for the XRD texture measurement is shown in Fig. 1b. In all cases it was the (0006) reflection which was scanned ($2\theta = 41.6°$, CuK_α radiation). The specimen tilt angles used were 0°, ±5°, and ±10°. These measurements differ from an earlier study [4], in that previously the axis of specimen tilt was perpendicular to the plane containing the incident and diffracted X-ray beams (the Y-axis in Fig. 1b). In the present experiments, the tilt axis is defined by the intersection of the plane of the specimen with the plane containing the incident and diffracted beams (the X-axis in Fig. 1b). Note that although at 0° tilt the whole of the irradiated area is in the focal plane of the X-ray detector, when tilted, most of the specimen lies either above or below this plane, thus leading to smearing of the observed diffraction peak. Further, if the region of the specimen lying in the focal plane is not in the center of the irradiated region, then the smeared peak will also appear displaced with respect to the 'ideal' Bragg position. However, providing all measurements are corrected for background noise and include the total, integrated number of counts under the recorded curve, then these defocus effects should not seriously affect the measured results.

Results

Table 1 summarizes the specimens studied and lists the relative densities (% of theoretical), where known, and the relative (0006) X-ray peak intensity at 0° specimen tilt (measured with respect to a specimen which contained no platelets). Specimens prepared without platelets (T33 and T3/4) were processed identically to those with platelets (that is, they were gel-cast, filter-pressed and sintered), in the one case with Ca^{2+} as the gelling cation, in the other with Sr^{2+}. T33 was used as a calibration specimen and assumed to be randomly oriented, so that all the relative intensities in Table 1 are expressed as the ratio I / I_{33}. The specimen T50 was conventionally processed by slip casting, and the texture in this specimen is associated with the fluid flow at the surface of the growing slip-cast cake.

The 0° tilt (0006) diffraction intensity data are given in histogram form in Fig. 2. In each case the plotted value is the average of the integrated peak intensities measured in 4 specimen configurations: namely, parallel and perpendicular to the original tape casting direction on both the top and bottom surfaces of the sample. The study revealed that for a given sample, the variations in texture between the different configurations were small (~ 5%), thus providing strong evidence that the texture is both uniform throughout the specimen, and symmetric about the normal to the sample.

A comparison of the diffractometer scans obtained for 3 different samples at different specimen tilt angles is given in Fig. 3. The bottom set of results is for an untextured sample (T33), for which the (0006) peak is only visible in the 0° tilt scan. The other two sets of results are for a moderately textured sample (top set, T30) and for a highly textured sample (middle set, T32). Both show extensive smearing of the peak profile with increasing tilt due to the loss of focus for those regions of the sample which are above and below the focal plane of the detector.

The integrated (0006) peak counts for these same two textured samples (T30 and T32) are shown as a function of the sample tilt angle in Fig. 4. The full-width, half-maximum of this c-axis distribution plot for both the samples corresponds to a deviation from the ideal c-axis texture of about ±5°. The sample prepared from the smaller alumina platelets (T32) has the higher peak intensity, suggesting that it contains a greater proportion of textured material than

the sample prepared from the larger platelets (T30).

Hardness indentation cracking observed on polished surfaces confirmed that the presence of a pronounced texture inhibited long-range crack propagation and promoted localized cracking in the neighborhood of the indentation [15]. Fig. 5a shows cracking associated with two 100 N indents in the untextured T33 specimen. The indents were made on a cross-section through the sample, and the indent diagonals were oriented at 0/90° and ±45° with respect to the specimen normal. It can be seen that the cracks are straight and originate primarily from the corners of the indentations. In contrast, for the highly textured sample (T32, Fig. 5b) the cracks are generally much shorter, and appear all around the indent, suggesting considerable mutual crack shielding. The same effect was observed in the less highly textured sample, T30, which again was indented in both the 0/90° and ±45° orientations (Fig. 5c).

More evidence for the strong effect of texture on the fracture process is given in Fig. 6. It can be seen that the fracture surface lies at an angle of approximately 45° to the specimen surface (Fig. 6a), and clearly shows the steps associated with the predominantly cleavage failure (Fig. 6b). Given that the preferred cleavage planes for alumina are $\{10\bar{1}2\}$ and $\{11\bar{2}3\}$ [17], both of which make an angle of approximately 35° to the basal plane, the present observations are entirely consistent with the expected angular distribution of the possible cleavage planes in a highly textured sample.

Micrographs taken from polished cross-sections of the samples confirmed that the textured samples had a sintered grain-size consistent with growth of the seed platelets into the surrounding fine-grained powder. If the platelet diameter is D and the volume fraction f then, for an aspect ratio A, the expected final grain size D_o is given by:

$$D_o = \alpha \, . \, D \, (\Pi / 4Af)^{1/3}$$

where α is a geometrical constant. Inserting f = 5vol%, D = 5μm, A = 7 and α = 1, we obtain D_o = 6.5μm, which is close to the observed grain sizes.

Fig. 7a shows the grain structure in a cross-section of the untextured material (T33), it can be seen that the slightly platelike grains appear randomly distributed. By comparison, the

highly textured sample (T32) has a much larger grain size, and the slightly non-equiaxed grains are preferentially oriented parallel to the sample surface (Fig. 7b). Pockets of highly porous, fine-grained material are visible, which strongly suggests that most of the residual porosity is associated with such regions. Comparison of the microstructures of T32 (highly textured) and T30 (moderately textured) demonstrate the rather interesting finding that there need not necessarily be an obvious correlation between the aspect ratio of the grains, and the degree of preferred orientation. The former pertains to the *microstructural texture*, whereas the latter is related to the *crystalline texture*. Further, the highly non-equiaxed and aligned grain structure of sample T30 (which was prepared from the larger platelets) shows that the original platelets were distributed in an anisotropic manner in the original tape. That is, if we consider the positions of the centers of gravity of the platelets, the platelet separation is much greater in the plane of the tape than in the through thickness direction.

Discussion and Conclusions

The gel-casting of powder slips containing alumina seed platelets results in a sintered monolithic product with a well-developed preferred orientation (crystalline texture). However, wide variations in the degree of texture (Table 1) have yet to be correlated with the size and volume fraction of the alumina platelets, the nature of the gelling cation, and the presence of other impurities and dopants.

There is a clear distinction to be made between microstructural texture (the presence of aligned non-equiaxed grains), and crystalline texture (preferred orientation). This is illustrated schematically in Fig. 8, which shows the expected microstructural effects of varying the volume fraction of the seed platelets and/or their size. Note that in every case it has been assumed that complete alignment is achieved (leading to an ideal 100% c-axis texture in the product). It can be seen that at low volume fractions, both small and large platelets will lead to an *equi-axed* microstructure (even though the crystalline texture is fully developed), since the seed platelets are expected to be isotropically distributed in the tape. The only difference will be in the scale of the microstructure; for a given volume fraction, there will be fewer platelets in the large platelet case, hence the grain size will be coarser.

At large volume fractions, the small platelets may still give rise to an equiaxed microstructure, assuming they are uniformly distributed in the green tape. However, due to geometrical considerations, large platelets must pack much closer together in the through-thickness direction, hence resulting in a highly non-equiaxed microstructure with aligned, plate-like grains. It is perhaps interesting to consider that whereas (as demonstrated in this study) it is possible to have strong crystalline texture in the absence of microstructural texture, because of the significant crystallographic influence on boundary mobilities, the converse case is much less likely.

The crack shielding features which have been observed in indented samples (Fig. 5) and the stepped nature of the cleavage-dominated fracture surface (Fig. 6) have both demonstrated the unusual failure characteristics of this material, but do not yet enable any clear prediction of the mechanical performance. Nevertheless, crack propagation in the through-thickness direction should be inhibited in the textured specimens, at least when compared to randomly textured samples of similar grain size. Furthermore, the comparatively large grain size of the textured alumina might be expected to lead to improved high temperature microstructural stability.

Finally, as mentioned previously, the thermal expansion coefficient of alumina parallel to the c-axis is approximately 10% greater than that in the perpendicular directions, leading to large residual microstresses in conventional monolithic aluminas. Thus an ideal c-axis texture should lead to an alumina which is free of thermal microstresses. Since such stresses are a common cause of failure in alumina-based ceramics, these textured materials may be expected to have a significant advantage for some applications.

Acknowledgements

The authors would like to acknowledge extensive discussions with Thierry Carisey (Technion), who also supplied the samples, as well as with Carol Handwerker (NIST). George Yasko was of immense practical help in performing the X-ray measurements. This work was funded by the Office of Naval Research and the authors would like to express their thanks to Steve Fishman (ONR) for his support and encouragement.

References

1. M. Farkash and D. G. Brandon, "Whisker Alignment by Slip Extrusion", Matls. Sci. Eng. [A], **177**, 269 (1994).

2. M. Farkash and D. G. Brandon, "SiC Whisker-Reinforced Ceramics With Modulated Microstructures", Matls. Sci. Eng. [A], **177**, 277 (1994).

3. S. Takagi, H. Yano, T. Oku, K. Shigeru, Y. Kuboto, and T. Shishikura, "Sintered Alumina Article With High Flexural Strength and Processing For Producing Same", U.S. Patent #4,996,177 (1991).

4. T. Carisey, A. Laugier-Werth, and D. G. Brandon, "Control of Texture in Al_2O_3 By Gel-Casting", J. Eur. Ceram. Soc. (in press).

5. R. Grylis, "Investigations Into Alignment of Discontinuous Reinforcement in Alumina", Materials Engineering Project Report, Technion, Haifa, Israel (1993).

6. I. Tsao and S.C. Danforth, "Injection Moldable Ceramic-Ceramic Composites; Compounding Behavior, Whisker Degradation and Orientation", Bull. Am. Ceram. Soc. 72 (1993) pp. 55-67

7. G.E.G. Bagg, M.E.N. Evans and A.W.H. Pryde, "The Glycerine Process for the Alignment of Fibers and Whiskers", 1 (1969) 97-100

8. N.J. Paratt, "Whisker Alignment by the Alginate Process", Composites 1 (1969) 25-27

9. N. Claussen and G. Petzow, "Whisker-Reinforced Zirconia Toughened Ceramics", in "Tailoring of Multiphase and Composite Ceramics", Eds. R.E. Tressler, G.L. Messing, C.G. Pantano and R.E. Newnham, Plenum Press, NY, 1986, pp. 649-62

10. S. Yamashita, H. Hatta, T. Sugano and K. Murayama, "Fiber Orientation Control of Short Fiber Composites: Experiment", J. Composite Materials 23 (1989) 32-41

11. E. Kragness, M. Amateau and G.L. Messing, "Processing and Characterization of Laminated SiC Whisker Reinforced Al_2O_3 Composites", J. Composite Materials 25 (1991) 416-432

12. M. Wu, G.L. Messing and M. Amateau, "Laminate Processing and Properties of Oriented SiC Whisker Reinforced Composites", in "Advanced Composite Materials", Ed. M. D. Sacks, Amer. Ceram. Soc. Westerville, OH, 1991 pp. 665-76

13. Y.S. Chou and D.J. Green, "SiC Platelet/Alumina Composites I: Effect of Forming Technique on Platelet Orientation", J. Am. Ceram. Soc. 75 (1992) 3346-52

14. M. Wu and G. L. Messing, "Fabrication of Oriented SiC Whisker Reinforced Mullite Matrix Composites by Tape Casting", J. Am. Ceram. Soc. (In Press).

15. T. Carisey, I. Levin, and D. G. Brandon, "Microstructure and Mechanical Properties of Textured Al_2O_3", J. Eur. Ceram. Soc. (submitted).

16. P. Chantikul, S.J. Bennison and B.R. Lawn, "Role of Grain Size in the Strength and R-Curve Properties of Alumina", J. Am. Ceram. Soc. 73 (1990) 2419-27

17. R. M. Cannon, pp. 818-38 in "Advances in Ceramics", Vol 10, ed. W. D. Kingery, American Ceramic Society, Columbus, OH, 1984.

Figure Captions

1. a) Jig and mount used for X-ray measurements.
   b) Schematic diagram depicting specimen geometry for measurements of preferred orientation.

2. Comparison of (0006) diffraction intensity data (0° tilt) for different specimens, where each value represents the average of integrated peak intensities measured in 4 different specimen configurations.

3. Comparison of diffractometer scans (at tilt angles of 0°, 5° and 10 °) for 3 different samples: a) T30 (moderately textured), b) T32 (highly textured), c) T33 (untextured).

4. Variation of (0006) peak intensity with tilt angle for samples T30 (dashed line) and T32 (solid line).

5. Comparison of indentation cracking morphology for: a) T33, 0/90° and ±45° orientation, b) T32 0/90° orientation, c) T30, 0/90° and ±45° orientation.

6. a) Fracture surface of tape-cast textured specimen (plane of surface oriented at ~ 45° to the casting direction).

   b) Higher magnification SEM micrograph showing cleavage within platelet grains.

7. SEM micrographs showing microstructure of: a) T33 (untextured), b) T32 (highly textured, c) T30 (moderately textured).

8. Schematic representation of dependence of grain size and microstructural texture on platelet size and volume fraction.

Table 1: Textured alumina specimen designations and data

Sample#	Platelet size, μm	Platelet vol.fract. %	Gelling cation	Dopant cation	Density, %theor.	Rel. XRD intensity
T33	-	none	Ca^{2+}	Cr+Mg	97.9	1.00
O+	-	none	Ca^{2+}	Cr+Mg	97.5	0.85
T50	3-7	2.5	Ca^{2+}	Cr+Mg	-	1.69
T32	3-7	5	Ca^{2+}	Cr+Mg	96.4	13.41
P+	3-7	5	Ca^{2+}	Cr+Mg	96.6	6.13
T30	10-15	5	Ca^{2+}	Cr+Mg	97.2	5.85
T37	10-15	10	Ca^{2+}	Cr+Mg	-	9.40
T3/4	-	none	Sr^{2+}	Mg	-	1.33
T49	3-7	2.5	Sr^{2+}	Mg	-	3.84
T47	3-7	5	Sr^{2+}	Mg	-	3.99
T48	3-7	10	Sr^{2+}	Mg	-	4.88
T38/2	10-15	10	Sr^{2+}	Mg	97.9	5.77
T38/3*	10-15	10	Sr^{2+}	Mg	97.0	4.12
T39	10-15	10	Sr^{2+}	Cr	97.2	4.16
T40	10-15	10	Sr^{2+}	Cr+Mg	96.5	6.40

* Specimen leached with dilute HNO_3 to extract gelling cation.

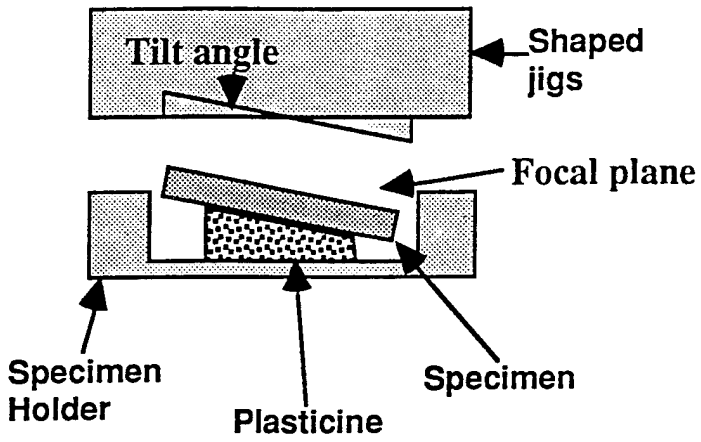

Fig.1a Jig and mount for X-ray measurements

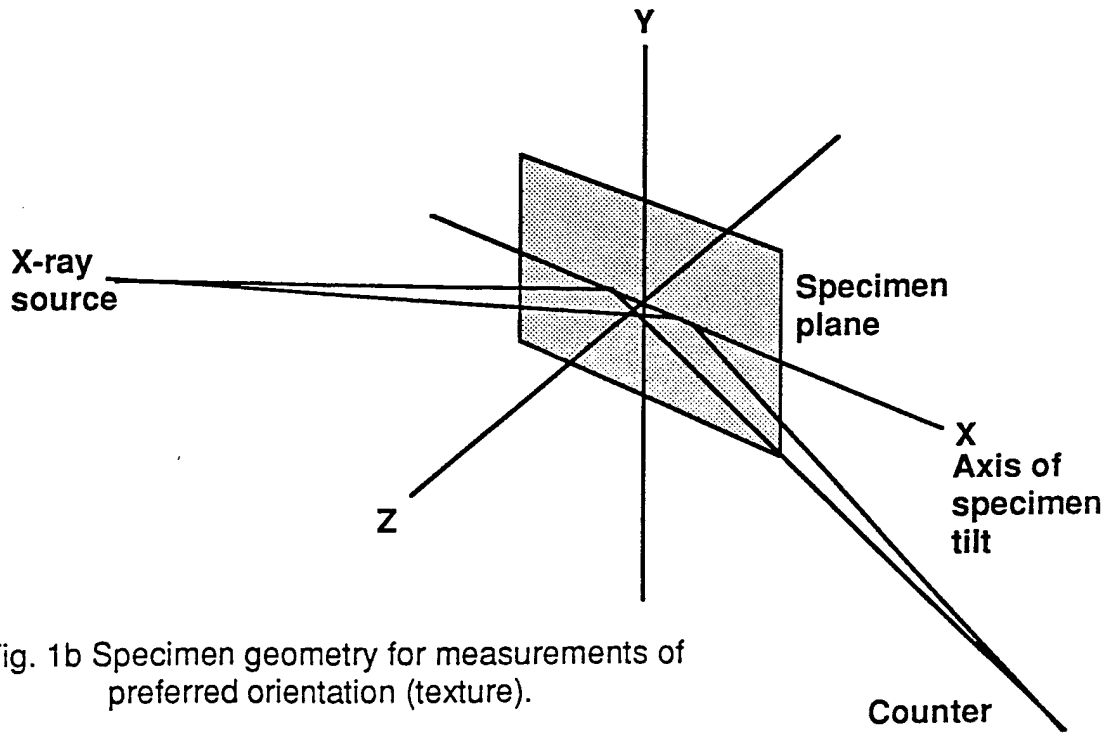

Fig. 1b Specimen geometry for measurements of preferred orientation (texture).

Fig 1

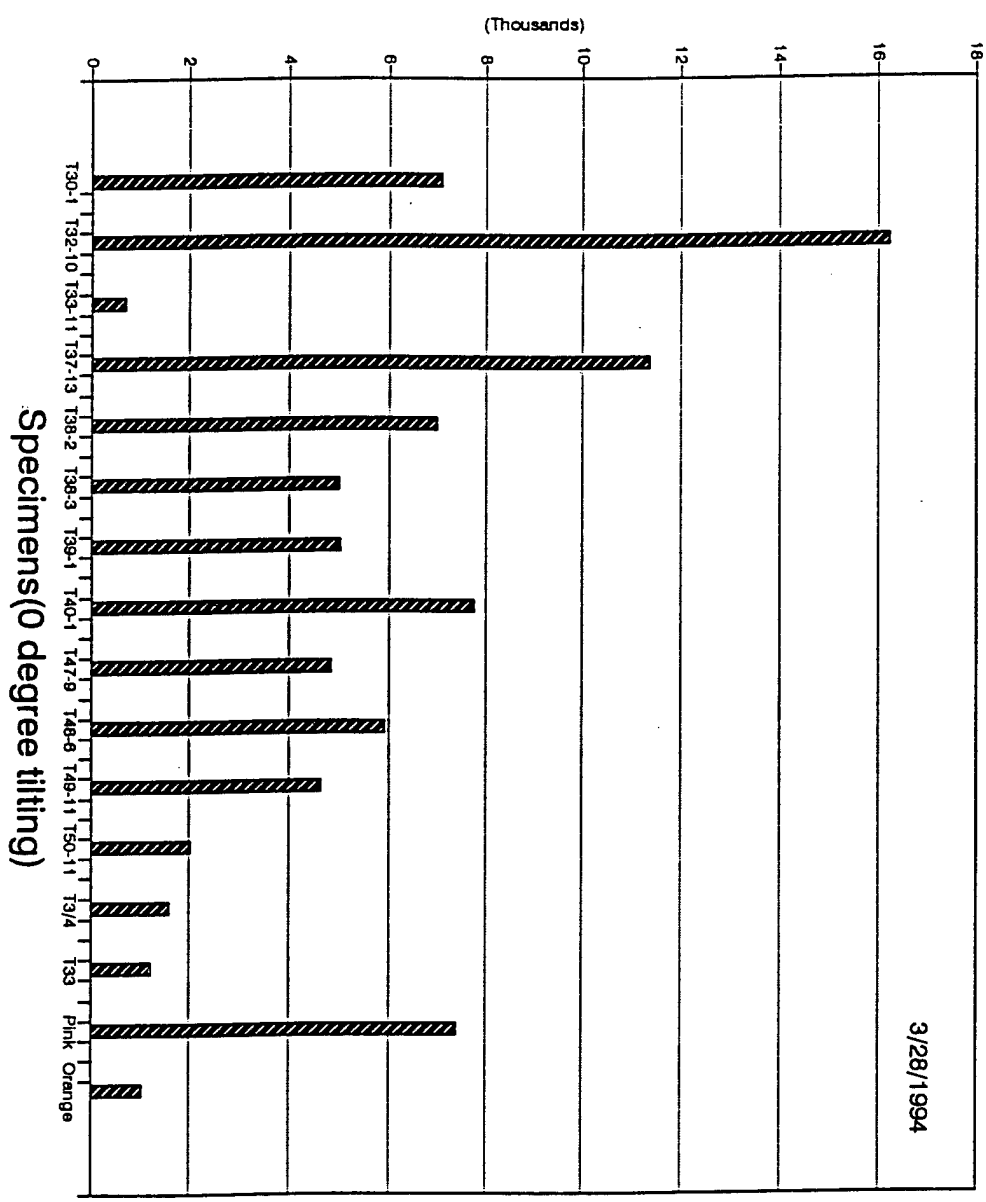
Average Diffraction Intensity(Counts)
(Thousands)
0
2
4
6
8
10
12
14
16
18
T30-1
T32-10
T33-11
T37-13
T38-2
T38-3
T39-1
T40-1
T47-9
T48-6
T49-11
T50-11
T3/4
T33
Pink Orange
Specimens(0 degree tilting)
3/28/1994

Fig 2

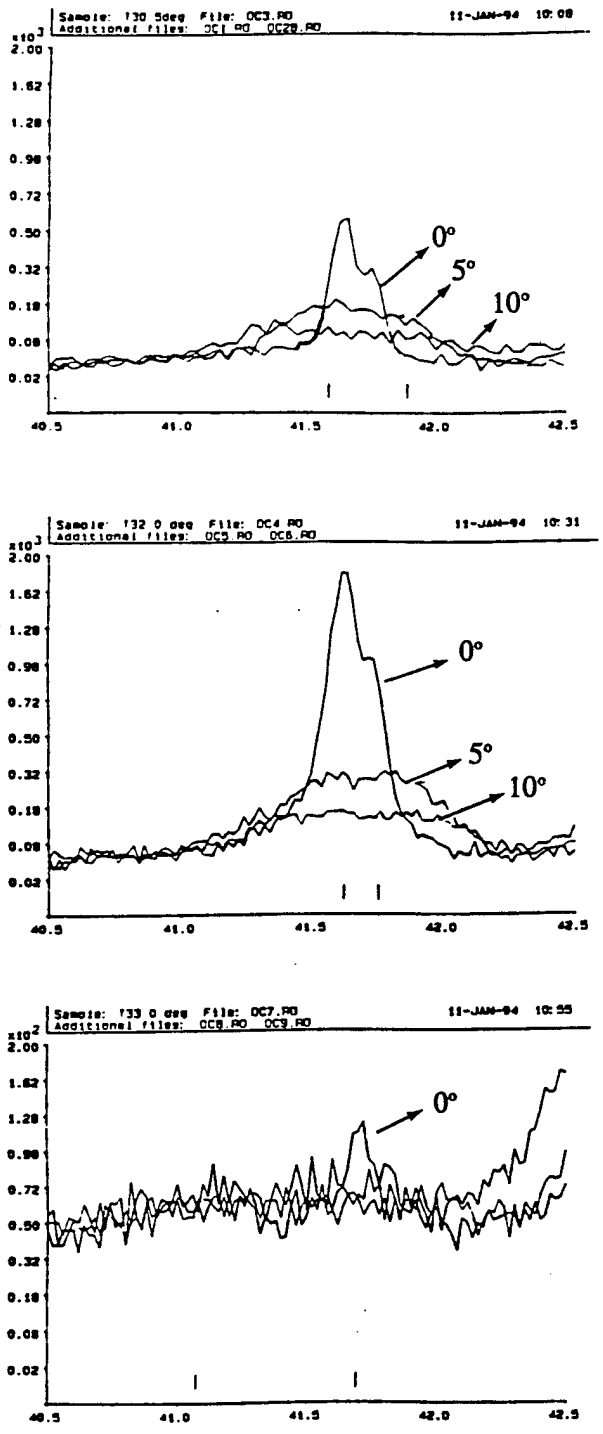

Counts

Diffraction Angle 2 Theta/degrees

Fig 3

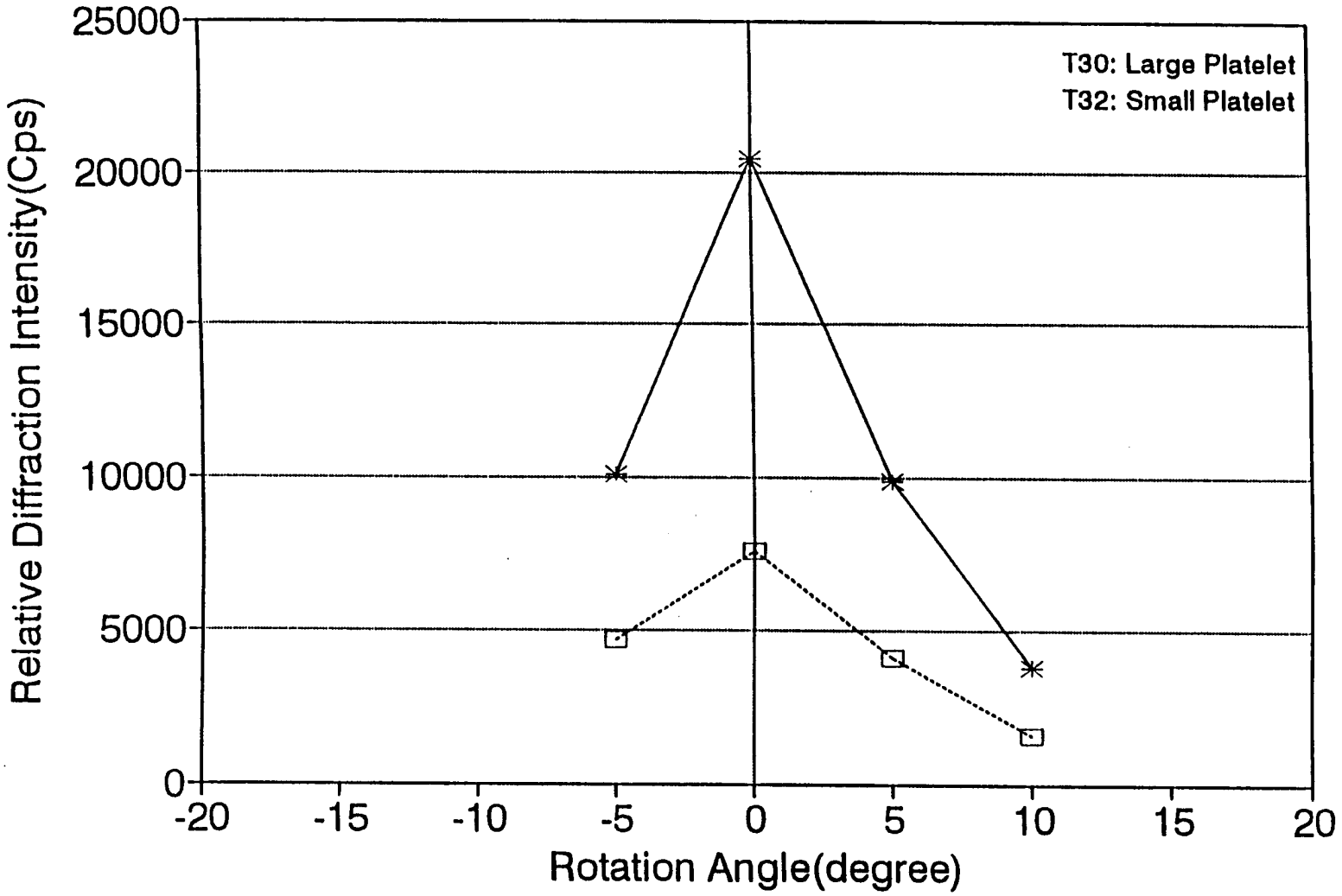
T30: Large Platelet
T32: Small Platelet
Relative Diffraction Intensity(Cps)
25000
20000
15000
10000
5000
0
-20
-15
-10
-5
0
5
10
15
20
Rotation Angle(degree)

Fig 4

A
100 μm
B
C

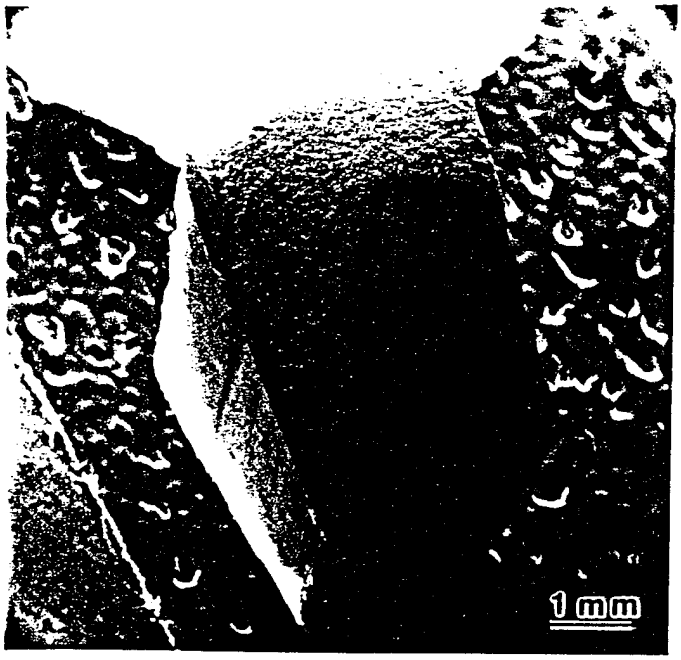
1 mm


20 μm

A
20 μm
B
C

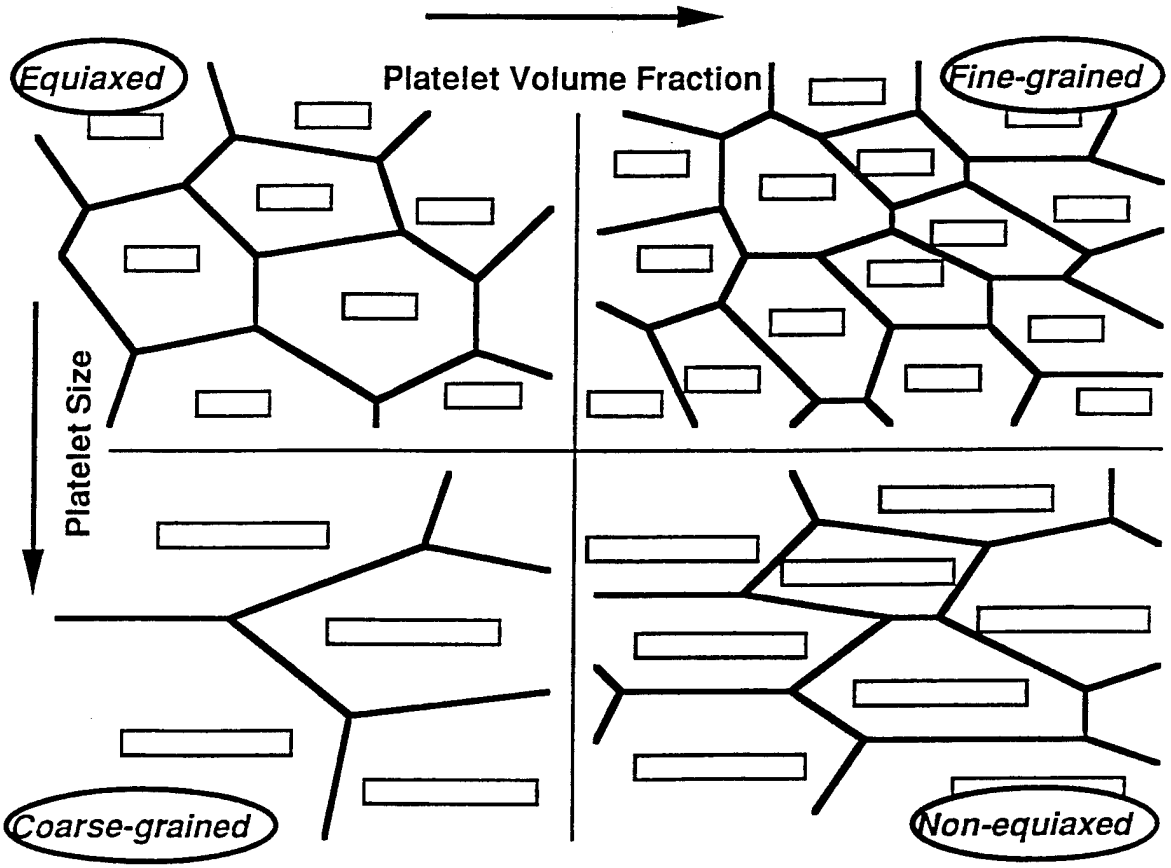
Platelet Volume Fraction
Platelet Size
Equiaxed
Fine-grained
Coarse-grained
Non-equiaxed

Fig 8

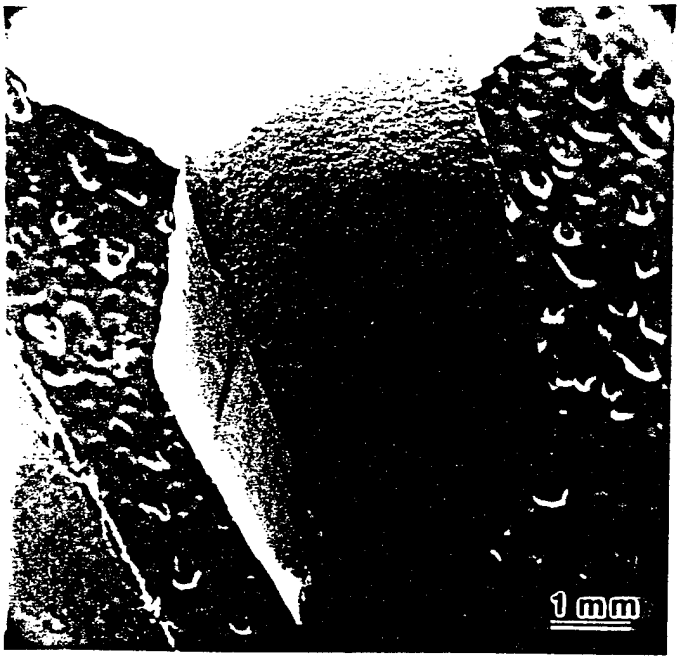
1 mm

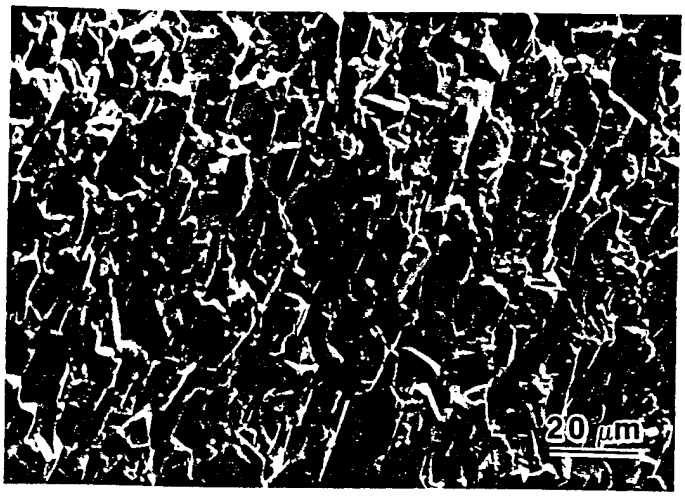
20 μm

OFFICE OF THE UNDER SECRETARY OF DEFENSE (ACQUISITION)
DEFENSE TECHNICAL INFORMATION CENTER
CAMERON STATION
ALEXANDRIA, VIRGINIA 22304-6145

IN REPLY REFER TO DTIC-OCC

SUBJECT: Distribution Statements on Technical Documents

TO: OFFICE OF NAVAL RESEARCH
CORPORATE PROGRAMS DIVISION
ONR 353
800 NORTH QUINCY STREET
ARLINGTON, VA 22217-5660

1995 1024 101

1. Reference: DoD Directive 5230.24, Distribution Statements on Technical Documents, 18 Mar 87.

2. The Defense Technical Information Center received the enclosed report (referenced below) which is not marked in accordance with the above reference.

FINAL REPORT
N00014-94-1-0037
TITLE: TOWARDS AN IN-SITU ALUMINA LAMINATE

3. We request the appropriate distribution statement be assigned and the report returned to DTIC within 5 working days.

4. Approved distribution statements are listed on the reverse of this letter. If you have any questions regarding these statements, call DTIC's Cataloging Branch, (703) 274-6837.

FOR THE ADMINISTRATOR:

1 Encl

GOPALAKRISHNAN NAIR
Chief, Cataloging Branch

FL-171
Jul 93

DISTRIBUTION STATEMENT A:

APPROVED FOR PUBLIC RELEASE: DISTRIBUTION IS UNLIMITED

DISTRIBUTION STATEMENT B:

DISTRIBUTION AUTHORIZED TO U.S. GOVERNMENT AGENCIES ONLY; (Indicate Reason and Date Below). OTHER REQUESTS FOR THIS DOCUMENT SHALL BE REFERRED TO (Indicate Controlling DoD Office Below).

DISTRIBUTION STATEMENT C:

DISTRIBUTION AUTHORIZED TO U.S. GOVERNMENT AGENCIES AND THEIR CONTRACTORS; (Indicate Reason and Date Below). OTHER REQUESTS FOR THIS DOCUMENT SHALL BE REFERRED TO (Indicate Controlling DoD Office Below).

DISTRIBUTION STATEMENT D:

DISTRIBUTION AUTHORIZED TO DOD AND U.S. DOD CONTRACTORS ONLY; (Indicate Reason and Date Below). OTHER REQUESTS SHALL BE REFERRED TO (Indicate Controlling DoD Office Below).

DISTRIBUTION STATEMENT E:

DISTRIBUTION AUTHORIZED TO DOD COMPONENTS ONLY; (Indicate Reason and Date Below). OTHER REQUESTS SHALL BE REFERRED TO (Indicate Controlling DoD Office Below).

DISTRIBUTION STATEMENT F:

FURTHER DISSEMINATION ONLY AS DIRECTED BY (Indicate Controlling DoD Office and Date Below) or HIGHER DOD AUTHORITY.

DISTRIBUTION STATEMENT X:

DISTRIBUTION AUTHORIZED TO U.S. GOVERNMENT AGENCIES AND PRIVATE INDIVIDUALS OR ENTERPRISES ELIGIBLE TO OBTAIN EXPORT-CONTROLLED TECHNICAL DATA IN ACCORDANCE WITH DOD DIRECTIVE 5230.25, WITHHOLDING OF UNCLASSIFIED TECHNICAL DATA FROM PUBLIC DISCLOSURE, 6 Nov 1984 (Indicate date of determination). CONTROLLING DOD OFFICE IS (Indicate Controlling DoD Office).

The cited documents has been reviewed by competent authority and the following distribution statement is hereby authorized.

A

(Statement)

OFFICE OF NAVAL RESEARCH
CORPORATE PROGRAMS DIVISION
ONR 353
800 NORTH QUINCY STREET
ARLINGTON, VA 22217-5660

(Controlling DoD Office Name)

(Reason)

(Controlling DoD Office Address, City, State, Zip)

DEBRA T. HUGHES
DEPUTY DIRECTOR
CORPORATE PROGRAMS OFFICE

(Signature & Typed Name)

(Assigning Office)

19 SEP 1995

(Date Statement Assigned)